ISSN 0020-4412, Instruments and Experimental Techniques, 2022, Vol. 65, No. 5, pp. 750–754. © The Author(s), 2022. This article is an open access publication, corrected publication 2023.
Russian Text © The Author(s), 2022, published in Pribory i Tekhnika Eksperimenta, 2022, No. 5, pp. 70–74.

ELECTRONICS AND RADIO ENGINEERING

Switches of Powerful Nanosecond Current Pulses Based on High-Voltage Units of Shock Ionized Dynistors

S. V. Korotkov[a,*], Yu. V. Aristov[a], and D. A. Korotkov[a]

[a] *Ioffe Institute, St. Petersburg, 194021 Russia*

**e-mail: korotkov@mail.ioffe.ru*

Received March 11, 2022; revised April 1, 2022; accepted April 2, 2022

Abstract—Monounit and modular switches of high-power current pulses with an operating voltage of 12 kV, made on the basis of series-connected shock ionized dynistors, are described. The switching processes of these switches are studied. The dependence of switching energy losses on the control pulse power is determined. The possibility of switching nanosecond current pulses with an amplitude of several kiloamperes at a frequency of several hundred hertz is shown.

DOI: 10.1134/S0020441222050074

Energy losses in switches of nanosecond current pulses are largely determined by the time of their switching. In this regard, the silicon semiconductor devices described in [1–4], which have different designs but switch in <1 ns, are of great interest. Such a short turn-on time is achieved as a result of using the method proposed in [5] for triggering by a high-voltage nanosecond pulse, which initiates the impact ionization of silicon. Current carriers created in the process of impact ionization provide high conductivity of semiconductor switches immediately after they are turned on.

This article presents the results of studies of high-power switches with a subnanosecond turn-on time, made in the form of units of series-connected shock ionized dynistors (SIDs), first described in [6]. As studies have shown [7, 8], a certain advantage of these dynistors is that their effective switching on can be provided by relatively low-power control circuits.

Figure 1 shows a diagram of the developed generator of powerful nanosecond pulses based on the C_0–R_0–L_0 power circuit and a SID unit with an operating voltage of 12 kV. Switching SID unit is carried out with the help of the control circuit of the CC containing the opening switch in the form of a high-voltage unit of drift diodes with sharp recovery (DSRD—drift step recovery diodes), first described in [9]. The nanosecond turn-off time of the DSRD unit is provided by a magnetic compression circuit based on a step-up transformer *Tr*, storage capacitor C_1, and transistor switch *Q* with an operating voltage of 1.2 kV.

The operation principle of the generator is as follows. In the initial state, the capacitors C_1 and C_0 are charged to voltage U_1 and U_0. Voltage U_1 is blocked by

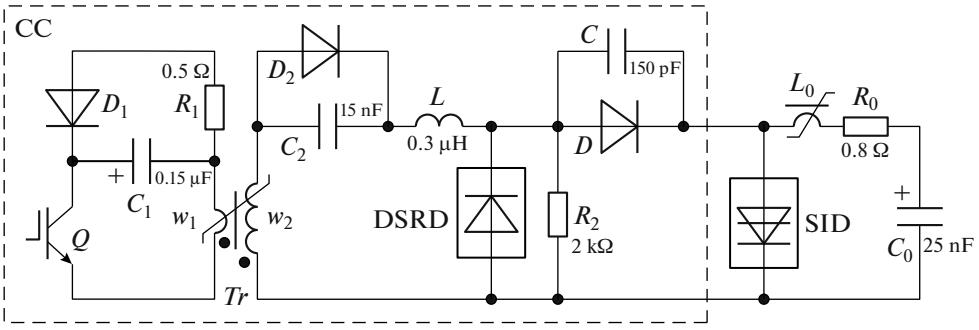

Fig. 1. Electrical circuit of the nanosecond pulse generator based on the SID unit. CC—control circuit; DSRD—25 diodes with a structure diameter of 16 mm; *D*—K100 (two in series); D_1—HER608; D_2—HER608 (four in series); *Q*—IRGPS60B120KDP (two in parallel); *Tr*—ferrite core N87 (EPCOS), eight rings measuring 25.3 × 14.8 × 10 mm, $w_1 = 1$, $w_2 = 3$; L_0—ferrite core N87 (EPCOS), five rings measuring 16 × 9.6 × 6.3 mm, $w = 1$.

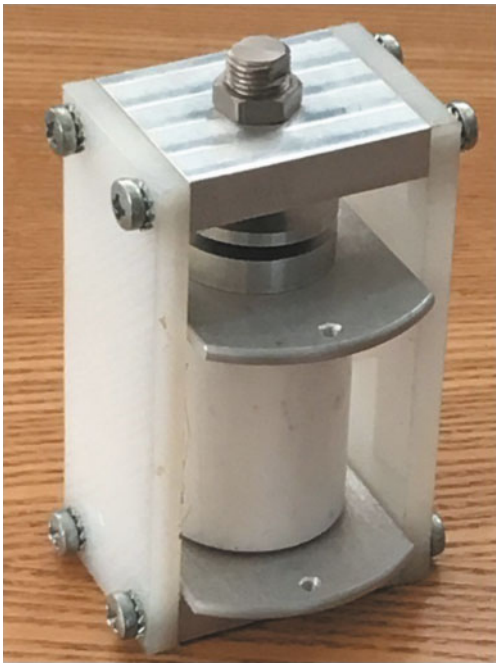

Fig. 2. SID unit with operating voltage 12 kV.

the key Q, voltage U_0 is applied to the SID unit and to the separating circuit C–D, which prevents the application of high voltage to the DSRD unit. After turning on the Q, capacitor C_1 is discharged through the primary winding w_1 of transformer Tr. As a result, current flows through the secondary winding w_2, which ensures the accumulation of charge in the diodes of the DSRD unit and the charging of the capacitor C_2. This current has a fundamentally short duration (~350 ns), which is necessary for efficient operation of the DSRD. At the end of the capacitor charging process of C_2, transformer core Tr is saturated. In this case, the inductance of the winding w_2 decreases sharply, and the capacitor C_2 is quickly discharged through the circuit L–DSRD–w_2. Current I_L flowing through inductance L removes the entire accumulated charge from the diodes of the DSRD unit in a time of ~150 ns. As a result, the diodes turn off synchronously in ~3 ns.

In the process of turning off the diodes, the voltage on the DSRD unit rises rapidly and is distributed between the circuit C–D, the SID unit, and the inductance of the installation wires that provide their connection. In this case, a control current I_c flows through the SID unit, and charges the dynistors' own capacitances that are close in value. When the voltage across the dynistors of the SID unit rises to a value sufficient to initiate the impact ionization process, they turn on.

When starting the SID unit, the choke L_0 has a large inductance, which, until the moment the dynistors are turned on, excludes the possibility of current I_c branching into the L_0–R_0–C_0 power circuit. After switching on the SID unit, capacitor charging voltage C_0 is applied to the choke L_0, and its core is remagnetized to saturation. After saturation of the core, the inductance of the choke decreases sharply, and the current in the power circuit rapidly increases. In the interval between the moment the SID unit is turned on and the moment the core of the choke L_0 is saturated, current I_c is flowing through the chain C–D and the SID unit, and modulates the conductivity of dynistors.

In our experiments, we used a small-sized SID unit with dimensions of 70 × 35 × 110 mm. It consisted of six series-connected dynistors, which had a diameter of 24 mm and a maximum permissible stationary voltage of 2.5 kV. A photograph of the SID unit is shown in Fig. 2.

The dynistors were placed in fluoroplastic cases. Flat plates were used for current supply. The electrical contact between the plates and dynistors was carried out by a clamping device based on massive duralumin plates fixed between caprolon plates. The clamping force was created by a central screw and stabilized with spring washers.

Figure 3 shows the voltage waveforms on the SID unit during its switching at different amplitudes of the current I_L, which was regulated by changing the charging voltage of the storage capacitor C_1. Oscillograms U_1, U_2, and U_3 correspond to the current I_L with an amplitude of 350, 250, and 200 A, respectively. They are obtained by using a resistor R_0 with a large resistance (1 kΩ), which eliminated the influence of the power current.

According to the oscillograms, at I_L = 350 A, the voltage rise rate on the SID unit is ~5 kV/ns. Under these conditions, the SID unit is switched on at a voltage of ~24 kV, which is 1.6 times higher than the total maximum allowable steady-state voltage of dynistors. The turn-on time of the SID unit is less than 1 ns.

When the current I_L decreases, the voltage rise rate on the SID unit decreases and is ~4 kV/ns at I_L = 200 A. At such a rise rate of the triggering voltage, the voltage across the SID unit decreases at the moment of its switching on and the turn-on time of the SID unit increases, apparently due to a decrease in the intensity of the impact ionization process.

In the process of research, the amplitude of the voltage pulse on the DSRD unit was measured. Due to the voltage drop in the circuit C–D and on the mounting inductance, it exceeded the voltage amplitude on the SID unit by 4 kV.

Figure 4 shows oscillograms of power current pulses (I_{01}, I_{02}) and voltage drop curves (U_1, U_2) on the SID unit calculated from the corresponding waveforms by subtracting the voltage dropped across the unit inductance. The experiments were carried out while charging the capacitor C_0 up to a voltage of 12 kV. Indices 1 and 2 denote currents and voltages obtained

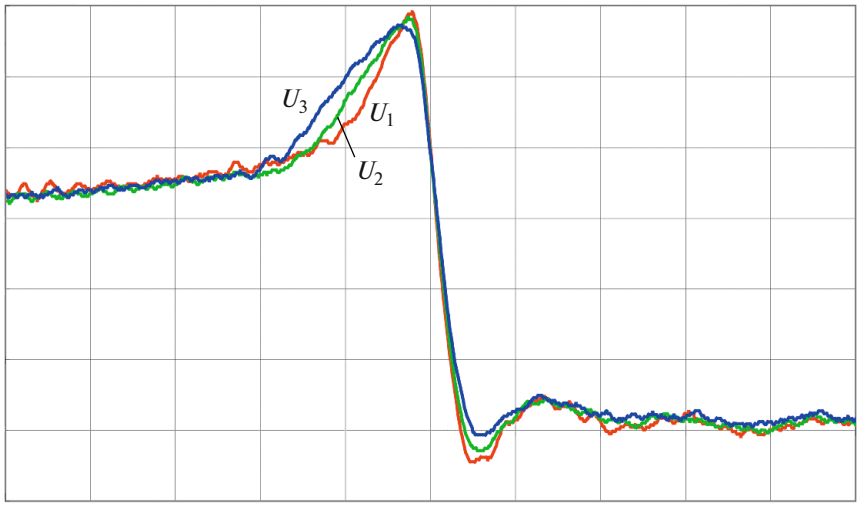

Fig. 3. Voltage waveforms on the SID unit at current I_L with an amplitude of 350 A (U_1), 250 A (U_2), and 200 A (U_3) Scale: vertical—4 kV/division; horizontal—2 ns/division.

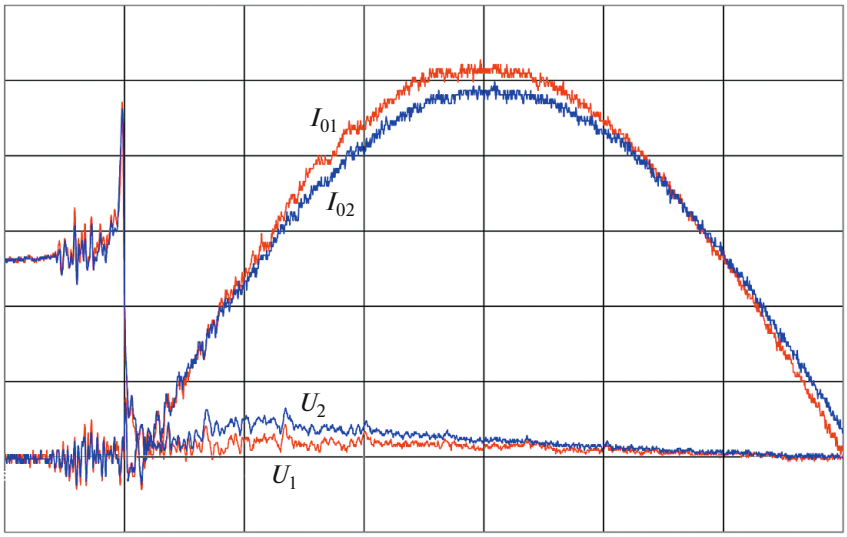

Fig. 4. Power current waveforms I_{01} and I_{02} and stress U_1 and U_2 on the SID unit at currents I_L with amplitudes of 350 and 250 A. Vertical scale: voltage—5 kV/division, current—500 A/division; horizontally—50 ns/division.

at currents I_L with an amplitude of 350 and 250 A, respectively.

The voltage on the SID unit was measured by a high-voltage divider capable of reliably measuring signals with a rise time of ≥0.5 ns. The divider was calibrated by measuring voltage pulses with a leading edge of 0.25 ns obtained using an I1-15 test pulse generator. The lower arm of the divider was a coaxial cable with a wave impedance of 50 Ω, and the upper arm was a small-sized resistor with a resistance of 470 Ω compensated by a copper screen. The divider was connected to the SID unit through a separating capacitor. For current I_0 measurement, the Pearson current monitor 410 current sensor was used.

As can be seen from Fig. 4, when the amplitude of the current I_L decreases from 350 to 250 A, the voltage drop across the SID unit increases significantly, which indicates a less uniform distribution of the power current over the area of the dynistors. With current I_L increasing from 350 to 450 A, the voltage drop across the SID unit remained practically unchanged, so we can assume that the current I_L with an amplitude of 350 A is optimal under the considered starting conditions. At this current I_L, energy losses in the SID unit when switching the current pulse I_{01} with an amplitude of 2.5 kA are approximately 320 mJ.

Such small energy losses determined the relatively low heating of the SID unit when switching current

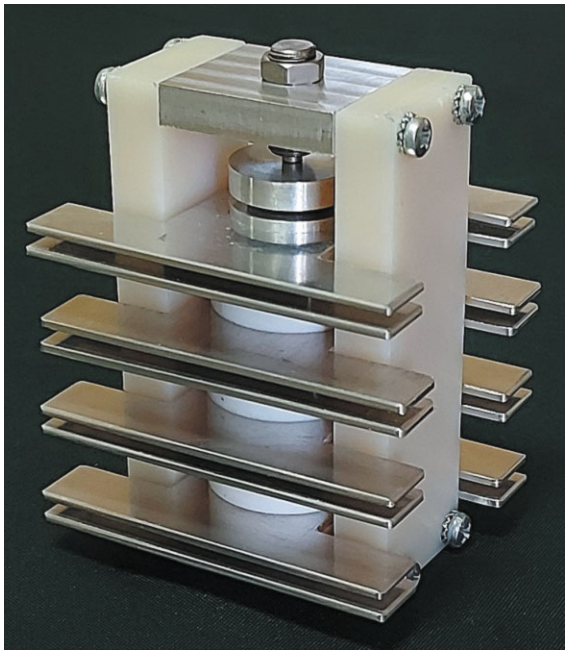

Fig. 5. Modular SID unit with an operating voltage of 12 kV.

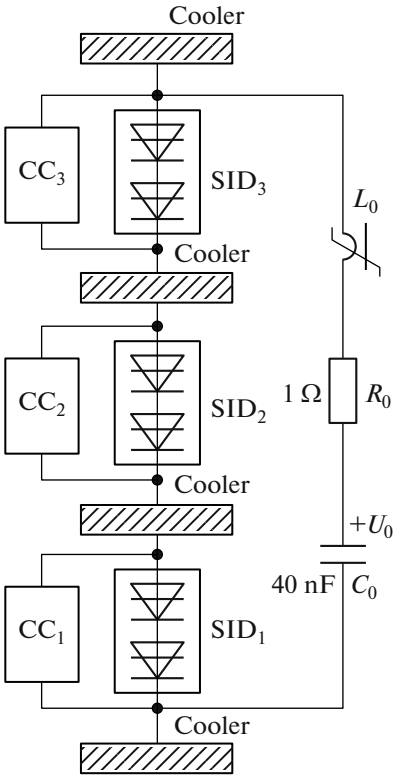

Fig. 6. Electrical diagram of the generator based on the modular SID unit. CC—control circuits; L_0—ferrite core N87 (EPCOS), eight rings measuring 16 × 9.6 × 6.3 mm, $w = 1$.

pulses I_{01} with a frequency of 150 Hz. When cooled by an air flow, the steady-state temperature of the SID unit case was ~70°C. Less heating of the SID unit can be achieved by using coolers pressed against the flat plates. At the same time, the dynistors in the central part of the unit will be cooled less intensively than the extreme dynistors.

More uniform heat dissipation from the dynistors was achieved by dividing the SID unit into three modules. Each module consisted of two dynistors connected in series. Coolers were placed between the modules. A photograph of a prototype SID unit of a modular design is shown in Fig. 5.

When the modular SID unit was started by the CC control circuit (see Fig. 1), the amplitude of the voltage pulses on the DSRD unit turned out to be excessively large (33 kV at a current $I_L = 350$ A). As a result, it was necessary to increase the number of diodes in the DSRD unit and take certain measures to increase the insulation strength of the transformer *Tr*. Such a high voltage was due to the relatively large inductance of the modular unit, which includes the inductance of the modules and the inductance of the coolers.

In this regard, a triggering scheme for the modular SID unit was developed, which is shown in Fig. 6. In this scheme, the switching of SID_1–SID_3 modules is carried out with the help of individual control circuits CC_1–CC_3 that turn on at the same time. Choke L_0 delays a sharp increase in power current for a time that exceeds the time spread of the moments of operation of the control circuits of the CC_1–CC_3. As a result, the switching of the delayed module occurs at a very low current in the power circuit, the influence of which can be neglected.

In the experimental SID-switch, the control circuits CC_1–CC_3 were constructed in the same way as the circuit CC in Fig. 1. They form current pulses I_L with the same amplitude (350 A). Since the SID_1–SID_3 modules have a low self-inductance and contain only two dynistors, the voltage on them at the moment of switching on is ~7.5 kV. At the same time, the voltage amplitude on the DSRD units used in the circuits CC_1–CC_3 does not exceed 9 kV, and only 10 diodes in series in each unit. Since a third of the voltage U_0 is applied to the modules in the initial state, only one K100 diode is used in separating circuits *C*–*D*. The considered structure of the modular switch made it possible to reduce energy losses in the CC_1–CC_3 circuits by 25% compared to the CC circuit in Fig. 1. As a result, efficient launch of SID_1–SID_3 modules was achieved at a lower charging voltage of storage capacitors C_1 and with smaller sizes of the transformers *Tr*.

When blown with air, the modular SID unit was able to switch current pulses with an amplitude of 3 kA and a duration of 400 ns, following at a frequency of 500 Hz. The studies were carried out without the selection of components in the control circuits of

CC_1–CC_3. In this case, the maximum spread of the moments of switching on the SID_1–SID_3 modules did not exceed 5 ns.

A certain advantage of the considered modular method for switching high-voltage SID units is that it allows intensive heat removal from dynistors when using coolers with large dimensions. At the same time, the relatively large intrinsic inductance of the coolers does not prevent the formation of nanosecond pulses for triggering dynistors.

Thus, the results of studies of the developed SID switches with an operating voltage of 12 kV indicate that they are able to effectively switch current pulses with an amplitude of several kiloamperes, which rise at a rate of tens of amperes per nanosecond. The operating principles of SIDs make it possible to significantly increase the operating voltage of SID switches and use them in nanosecond pulse generators with an average power of several kilowatts.

OPEN ACCESS

REFERENCES

1. Efanov, V., Kardo-Sysoev, A., Tchashnicov, I., and Yarin, P., *Proc. 22nd Int. Power Modulator Symposium,* Boca Raton, FL, 1996, p. 22. https://doi.org/10.1109/MODSYM.1996.564440
2. Grekhov, I., Korotkov, S., and Rodin, S., *IEEE Trans. Plasma Sci.,* 2008, vol. 36, no. 2, part 1, p. 378. https://doi.org/10.1109/TPS.2008.918661
3. Korotkov, S.V., Aristov, Yu.V., Voronkov, V.B., Zhmodikov, A.L., Korotkov, D.A., and Lyublinskii, A.G., *Instrum. Exp. Tech.,* 2009, vol. 52, no. 5, pp. 695–698. https://doi.org/10.1134/S0020441209050091
4. Gusev, A.I., Lyubutin, S.K., Rukin, S.N., and Tsyranov, S.N., *IEEE Trans. Plasma Sci.,* 2016, vol. 44, no. 10, part 1, p. 1888. https://doi.org/10.1109/TPS.2016.2542343
5. Grekhov, I. and Kardo-Sysoev, A., *Sov. Tech. Phys. Lett.,* 1979, vol. 5, no. 8, p. 395.
6. Korotkov, S.V., Aristov, Yu.V., and Voronkov, V.B., *Instrum. Exp. Tech.,* 2019, vol. 62, no. 2, pp. 165–168. https://doi.org/10.1134/S0020441219010111
7. Korotkov, S.V., Aristov, Yu.V., Zhmodikov, A.L., and Korotkov, D.A., *Instrum. Exp. Tech.,* 2020, vol. 63, no. 5, pp. 683–688. https://doi.org/10.1134/S0020441220050176
8. Korotkov, S.V., Aristov, Yu.V., Korotkov, D.A., and Zhmodikov, A.L., *Rev. Sci. Instrum.,* 2020, vol. 91, p. 084704. https://doi.org/10.1063/5.0015284
9. Grekhov, I., Efanov, V., Kardo-Sysoev, A., and Shenderey, S., *Solid-State Electron.,* 1985, vol. 28, no. 6, p. 597.